The relationship between surface area and roughness of 3D printed highly structured anode surfaces for application in a Microbial Fuel Cell (MFC)

J.W. McBride[1,2], T.G Bull[1], Y.Yang[2], C. Chianrabutra[3]

[1]Mechanical Engineering, University of Southampton, UK; [2]TaiCaan Technologies Ltd. Southampton, UK; [3]Mechanical Engineering Kasetsart University, Thailand.

The anode surface area and surface roughness of a Microbial Fuel Cell (MFC) are key performance parameters, as they link to the power density and the voltage produced by the cell. In this study 3D printed carbon-based anodes with pyramid structures are investigated to determine the influence of texture and structure on surface area. The dimensions of the base area of the 3D printed pyramids are typically 2 x 2 mm with apex heights between 1.5 and 2.0 mm. The surfaces are measured using confocal scanning. The characterisation of these highly structured surfaces is dependent on the optical measurement systems ability to return valid data from a highly sloping surface. A methodology is developed for the measurement of the local surface roughness of the features. The 3D printed surfaces are shown to have a local pyramid side wall roughness (Sa) of 60 to 100 µm, which is shown to increase the surface area of the electrode.

Keywords: Optical Metrology, Anode surfaces for Fuel Cell, Microbial Fuel Cell, Surface Area and 3D roughness.

Introduction

A Microbial Fuel Cell (MFC) is a method of generating electricity via biomass using bacteria, where chemical energy is converted from organic wastewater into electrical energy using electro-chemically active microorganisms. MFCs utilise the bio-catalytic capabilities of microorganisms capable of oxidizing a wide range of organic fuels, breaking them down into carbon dioxide, hydrogen ions and electrons. MFCs low power density output is a limiting factor preventing the development of wider applications [1]. The aim of this work is to explore surface characterisation of 3D printed electrodes with highly structured surfaces of varying heights, using BEX® surface characterisation software on samples measured using Confocal Scanning (CFS) [2]. A highly structured surface is defined as a surface where the height of the features in the Z axis is of the order of their lateral dimension in the XY plane [3]. Structured surfaces with pyramid features, an example of which is shown in Fig.1, are investigated with varying pyramid heights of 1.5 to 2.0 mm, to determine the link to surface area and local surface roughness.

Most investigations into structured surfaces [4,5] use top-down single frame areal metrology limited by the field of view (measurement area) and the angular tolerance of the sensing method. In [4,5] the surfaces studied were nominally flat surfaces where the features are much smaller in height than their lateral plane dimensions. Highly structured surfaces were studied in [6,7] with investigation of the grooved surfaces of historical mechanical sound recordings where the height of features is of similar dimension to the width of features. In these studies, large area surfaces (more than 2500 mm^2) were measured using Con-Focal Scanning (CFS), where a point sensor is scanned across the large area of the surface. The CFS method allows for higher precision on large area measurement when compared to the single frame areal metrology where the large areas can only be measured by data stitching. The CFS method has the additional benefit that it can easily be applied to rotational objects such as discs and cylinders. Many of the recordings studied in [6,7] were cylinder recordings. The typical vertical resolution of the sensors used in these studies was 10 nm with the limiting factor in measuring the highly sloped surface regions being the angular tolerance of the sensors.

The angular tolerance of the optical sensor is critical for measurement of a highly structured surface and linked to the ability of the optical sensing method to return a valid signal from a sloped, non-specular surface. A surface perpendicular to the light source is defined as a 0° slope surface, (horizontal), while a 90° surface (vertical) is aligned with the source. A vertical surface is unable to reflect the incident light from the CFS sensor and as such cannot be measured by any confocal optical system, but the edge features have been shown to be detectable to a high precision for dimensional metrology purposes [8]. Coordinate Measurement Machines (CMM) can used to measure vertical walls using a touch probe, but these systems give insufficient spatial resolution surface data of texture. X-Ray Computed Tomography (X-CT) have been used to measure surface data but with limited accuracy and precision [9].

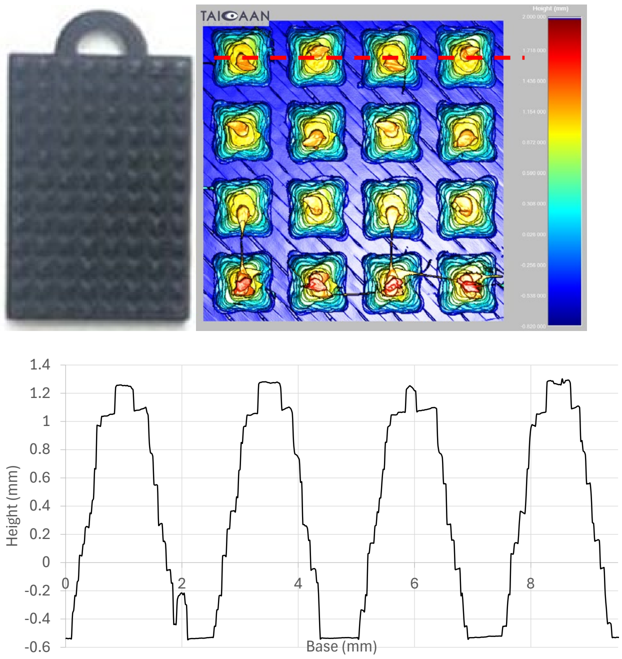

Fig. 1. 3D printed Carbon Anode (top left) with CFS colour scaled image (top right) over 10 x 10 mm region of printed structure with vertical colour scale from 2.0 to -0.82 mm. Data source; 2.6mm horizonal printed with grid data spacing δ = 20 µm. (lower) Cross section as indicated in top right.

Methods

An example 3D printed sample is shown in Fig.1 (top left), with a measured surface using a XYRIS Ultra 2020H instrument, (top right). The measurement instrument is a calibrated 3 axis CFS system, with a large area measurement capability of 200 x 200 mm and an ultra-flat motion system, and a form error of less than 0.1 µm over the motion area. The sensor used has a high gauge range (3 mm) with 30 nm resolution and a high angular tolerance of >70° as shown in Fig.1 (lower) where a cross section measurement across the top four pyramids in Fig 1 (upper right dashed red line) shows the pyramid side wall slope of 60 - 70°. The 3D printed anode surfaces are typically 20 x 30 mm, while Fig.1 (top right) shows an example surface measured over 10 x 10 mm selected to highlight printing defects associated with a horizontal (bottom up) print of surface. The colour scale indicates the height of the features. The cross section of features shown in Fig.1 (lower) are 1.8 mm above the base, with each structure typically with a base dimensions of 2 x 2 mm. Fig.1 shows several of the pyramids have printing defects with printed filaments connecting adjacent peaks (stringing defects).

Study 1: **Determination of the local areal surface roughness.** To find the local roughness of the surface a 2D method could be used where the 2D cross section as shown in Fig.1 (lower) is processed. To find the areal roughness however requires the form of structured features to be removed so that the local roughness is determined relative to a defined zero mean plane. This latter approach has been enhanced using the BEX® software with the ability to undertake regional surface roughness mapping (RSa) [10]. The RSa methods creates a map of the roughness (Sa) where the local Sa is calculated over a circular region of a user defined radius for each data point in the measured data. The method required a two-step process.

1. Apply a 3D Gaussian filter to the surface to remove the form features below the cut-off length. In this study the features are typically 2 x 2 mm so a 0.8 mm filter length is applied.
2. Apply the RSa method over a region of radius 0.25 mm. The user selected radius is determined here to be lower than the Gaussian filter length, and greater than the step feature size on the side walls of the pyramid structure as shown in Fig.1. The filter radius selected is 1/8 of the base dimension. Varying the radius will provide slight variation in the mapping and processing time.

Study 2: **The relationship between the measured average pyramid heights and surface area**. A ratio of the 3D measured surface area to the 2D projected surface area is used to normalise area measurement. The calculation is based on a selected region of the 3D printed surface with an array of 3 x 3 pyramids with little or no printing defects. In Fig.1 the top left 3 x 3 array is used. The surface area ratio will always be greater than 1 and will increase with the height of the pyramids. The measured surface area is compared to the theoretical value for texture-less (smooth) pyramids defined as the minimum surface area ratio.

Results

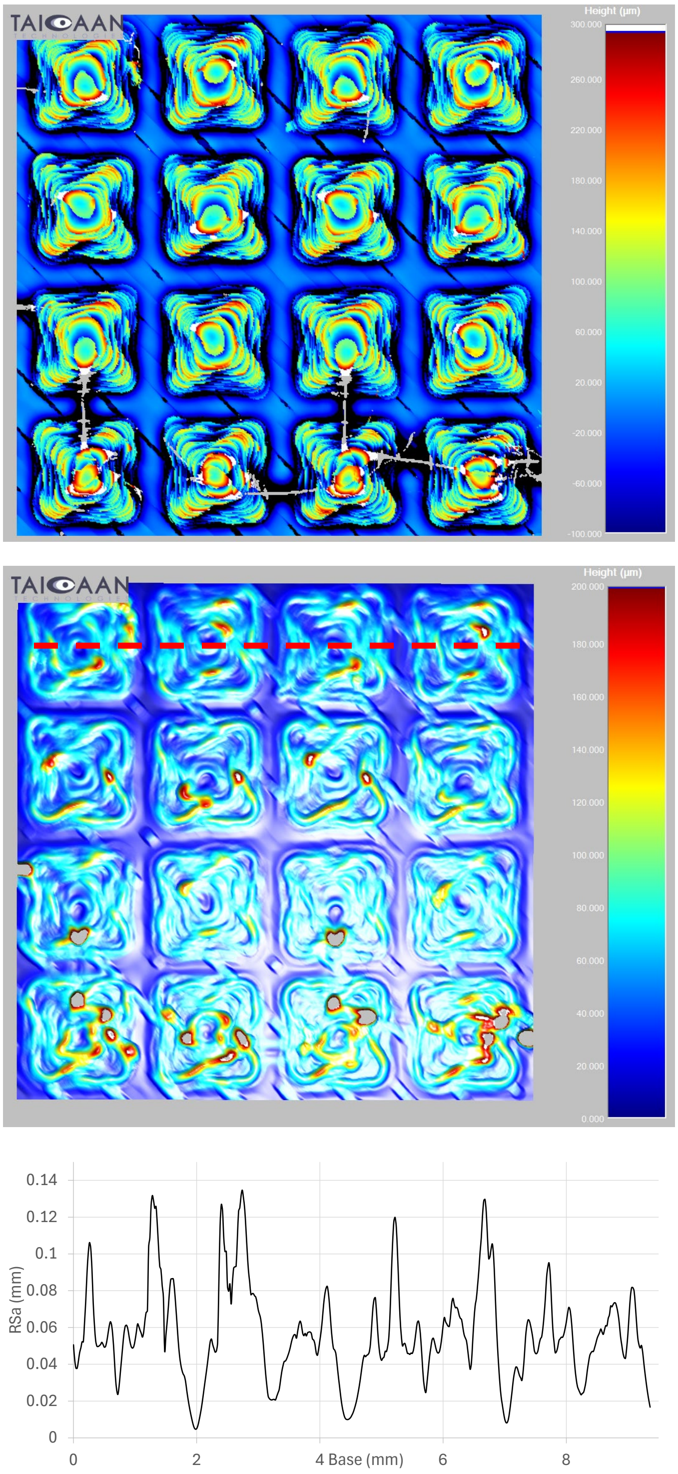

Fig 2. (upper) 0.8 mm Gaussian filter applied to the data in Fig 1(upper) with colour scale 0.3 to -0.1 mm; (middle) regional surface roughness mapping function RSa 0.25mm; (lower) RSa for cross-section as in Fig.1 (lower).

Study 1. Fig.2 shows the local surface roughness for the sample shown in Fig.1 using the method defined. In the upper image the surface is first levelled by the application of a 0.8 mm Gaussian filter, with the colour scale between +300 and -100 µm. The base of the pyramids are at approximately 0 (blue) while the highest features (red) are on the side walls of the pyramids, with features of 300 µm above the zero base. The data has been cut off to a maximum of + 300 µm to remove the stringing defects that can be seen in Fig.2 (upper) coloured grey and linking pyramid peaks along the lower rows.

The application of the RSa filter with a defined radius of 0.25 mm is shown in the Fig.2 (middle) where the colour scale corresponds to the local Sa roughness, from 0 to 200 µm. Fig.2 (lower) shows the variation of the RSa along a cross section shown in the upper figure and corresponding to the cross section shown in Fig.1. The Sa for the side walls of the pyramids is shown to be 60 - 130 µm, consistent with the data in Fig.1. This high level of roughness of the side walls is associated with the quality of the printing process and is a design advantage for the MFC application. The enhanced roughness of the side walls of the structure will act to enhance the surface area which will increase the effectiveness of the MFC in terms of electrical power generation. For the base around the pyramid structures the roughness is much lower than the side walls with a range 5 to 40 µm, for the cross-section shown in Fig.2.

Study 2. Six, 20 x 30 mm Polylactic Acid (PLA) graphite filament composite electrode samples with varying pyramid heights were printed and measured. The sample shown in Fig.1 has a designed height of 2.6 mm. For this sample the average height over a selected 3 x 3 peaks without printing defects is 1.78 mm as shown in the cross section of Fig.1 (lower). The difference between the design height and the measured height is linked to the difficulty in printing the fine detail of the pyramid tip structure. For the data the average measured heights are used.

To find the average pyramid height, the array of 3 x 3 pyramid with fewest defects were selected from the measured data and used for the surface area ratio calculation. The results are shown in Fig.3 for horizontal printing. The minimum area ratio is calculated for a 2 x 2 mm pyramid base where the surfaces are smooth. The minimum value for the area ratio (not shown in the figure) is for pyramids of height zero and the ratio is 1. The measured data shows that the contribution of surface area increase from texture increases with average pyramid height.

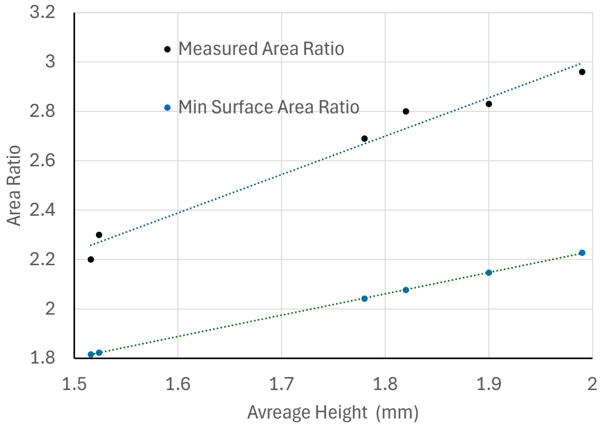

Fig. 3 Study 2. The ratio of the pyramid surface area with the average pyramid height

Discussion

The regional surface roughness mapping (RSa) in Fig.2 for the sample shown in Fig.1 shows that the roughness is linked to the horizontal layering of the 3D printer. This is also shown in the steps on the side wall of the pyramid cross section in Fig.1 (lower). For this sample the average height is 1.78 mm and in Fig.3 the corresponding area ratio for a subset of 3 x 3 peaks is 2.7. This implies that for the MFC application the surface area for interaction with the microbial actions would 270% greater than a perfectly flat surface. Further, the surface roughness of the side walls of the pyramid leads to an additional 32% increase in surface area over a perfectly flat side wall. The corresponding functional anode area for voltage and current generation would therefore also be greater. Following this it is apparent that by increasing the measured average height of the pyramid structure to 2 mm would provide an area ratio of 3, an increase of 35% in surface area.

Fig.3 also shows that as the measured average height of the pyramids increase, the surface area ratio appears to be increasing at a greater rate than the minimum surface area ratio, as shown by the divergence of the two best fit lines.

There will be a limit to the benefits of increasing the height of the pyramids, since as the height increases the side wall will become increasingly perpendicular and the added benefit of the roughness caused by the horizontal layering during printing will be expected to reduce.

The long-term interaction of the active microorganisms with the printed surfaces is not considered in this work and would be expected to be linked to liquid flow within the MFC structure.

Conclusions

An analysis of the surface roughness of a highly structured 3D printed surface using regional surface roughness mapping (RSa) shows the side wall of a pyramid structure having a much higher roughness than the printed base.

The relationship between the manufactured height of the pyramid structure and the surface area shows that the roughness enhances the magnitude of the surface area and that as the height of the pyramids increases the side wall roughness increases. The surface roughness of the side wall of the pyramids increases the surface area by 35% for a 2 mm high pyramid on a 2 x 2 mm base, when compared to a perfectly smooth side wall.

References

1. T. Kulchartvijit, C. Chianrabutra, S. Sukontasing, S. Chianrabutra, “The Effects of Surface Roughness of the Stainless-Steel Anode on Electricity Enhancement of Microbial Fuel Cell”, TRENDS IN SCIENCES 2022; 19(9): 3680.
2. J.W.McBride “Confocal-Scanning of Surfaces”, Metrology Letters Guide, 2020.
3. J.W. McBride, K.J. Cross, ‘The surface area and localised 3D roughness of a highly structured surface using X-Ray Computed tomography (XCT)’. Metrology Letters, 2020.
4. N. Senin, L.A. Blunt, R. K Leach, S Pini, “Morphologic segmentation algorithms for extracting individual surface features from areal surface topography maps”. Surf. Top. Metrol. Prop. 1 (2013) 015005 pp1-11.
5. G MacAulay, Ph.D Thesis, “Characterisation of structured surfaces and assessment of associated measurement uncertainty”, 2015.
6. P.J. Boltryk, M. Hill, J.W. McBride, A. Nasce, “A comparison of precision optical displacement sensors for the 3D measurement of complex surface profiles”, 2008, Sensors and Actuators A: Physical, 142, (1), 2-11.
7. P.J. Boltryk, Hill M, McBride, J.W. “Comparing laser and polychromatic confocal optical displacement sensors for the 3D measurement of cylindrical artefacts containing microscopic grooved structures”, 2009, Wear, 266, (5-6), 498-501.
8. J.W. McBride, T.G. Bull, “An optical CMM system for nominally flat surfaces with sub-micron precision”, Metrology Letters, 2023.
9. J.W. McBride, K.J. Cross, “Segmentation and surface roughness mapping applied to optical, and X-Ray CT measured free-form dental surfaces subjected to acidic erosion”, Metrology Letters, 2024.